# Relationship between hole density and charge-ordering wave vector in $Sr_{14-x}Ca_xCu_{24}O_{41}$

A. Rusydi,[1,2,3] M. Berciu,[4] P. Abbamonte,[1,5] S. Smadici,[1,5] H. Eisaki,[6] Y. Fujimaki,[7] S. Uchida,[7] M. Rübhausen,[3] and G. A. Sawatzky[4]

[1]*National Synchrotron Light Source, Brookhaven National Laboratory, Upton, New York 11973-5000, USA*

[2]*Materials Science Centre, University of Groningen, 9747 AG Groningen, The Netherlands*

[3]*Institut für Angewandte Physik, Universität Hamburg, Jungiusstraße 11, D-20355 Hamburg, Germany*

[4]*Department of Physics and Astronomy, University of British Columbia, Vancouver, British Columbia V6T-1Z1, Canada*

[5]*Physics Department and Frederick Seitz Materials Research Laboratory, University of Illinois, Urbana, Illinois 61801, USA*

[6]*Nanoelectronics Research Institute, AIST, 1-1-1 Central 2, Umezono, Tsukuba, Ibaraki 305-8568, Japan*

[7]*Department of Superconductivity, University of Tokyo, Bunkyo-ku, Tokyo 113, Japan*

(Received 20 October 2006; published 21 March 2007)

The distribution of holes in $Sr_{14-x}Ca_xCu_{24}O_{41}$ is revisited with semiempirical reanalysis of the x-ray absorption data and exact diagonalization cluster calculations. Another interpretation of the XAS data leads to much larger ladder hole densities than previously suggested. These new hole densities lead to a simple interpretation of the hole Wigner crystal recently reported with 1/3 and 1/5 wave vectors along the ladder. Our interpretation is consistent with paired holes in the rung of the ladders. Exact diagonalization results for a minimal model of the doped ladders suggest that the stabilization of spin structures consisting of 4 spins in a square plaquette as a result of resonance valence bond physics suppresses the hole crystal with a 1/4 wave vector.

DOI: 10.1103/PhysRevB.75.104510 PACS number(s): 74.25.Jb, 71.10.Li, 73.20.Qt, 78.70.Dm

## I. INTRODUCTION

$Sr_{14-x}Ca_xCu_{24}O_{41}$ (SCCO) is a layered material consisting of two different types of copper oxide sheets—one with $CuO_2$ "chains" and one with $Cu_2O_3$ "ladders" (see Fig. 1).[1,2] The sheets are separated by Sr/Ca atoms, and are stacked in an alternating fashion along the *b* crystallographic direction. These layers are structurally incommensurate, the ratio of chain and ladder lattice constants being $c_c/c_L \approx 7/10$. (The low-temperature lattice parameters[3] are $a=11.47$ Å, $b=13.35$ Å, and $c=27.3$ Å $\approx 7c_L \approx 10c_c$.) From charge neutrality, the formal valence of Cu is +2.25, resulting in six holes per unit cell if counting from a $Cu^{2+}$ state. The substitution of isovalent Ca for Sr redistributes the holes between the chains and the ladders without changing the total hole density. This allows the investigation of the properties of two-leg ladders at different hole densities, and in the absence of strong scattering by charged impurities which complicates issues in other doped systems.

A hole-doped two-leg spin ladder is the minimum model needed to obtain superconductivity (SC),[2,4,5] although this phase competes with an insulating hole Wigner crystal (HC) phase.[4,6,7] Superconductivity with $T_C \approx 12$ K has indeed been found by Uehara *et al.* for samples with $x=13.6$ under hydrostatic pressure larger than 3 GPa.[8] Recently, using resonant soft x-ray scattering (RSXS), the HC phase in the ladders was also discovered.[9,10] However, the HC is observed only for odd periodicity. As the hole density is varied, the HC forms with the commensurate wave vectors $\lambda_{HC}=5c_L$ $(x=0)$ and $\lambda_{HC}=3c_L$ $(x=11)$ but for other values it melts. The competition between the HC and SC phases in the two-leg spin ladder is believed to be similar to that between ordered stripes and SC in doped two-dimensional Mott insulators,[11] making it an important model system to try to understand. In fact, a two-dimensional model of coupled two-leg spin ladders[12] was used to explain recent neutron scattering data of cuprates.[13]

A serious problem exists, however, in understanding the periodicity of the HC in terms of what is thought to be the correct doped hole density of the ladders (see below). The often accepted distribution of the six holes per unit cell is into $n_L \approx 1$ on the ladder and $n_c \approx 5$ on the chain. For the ladder, this means a hole density of about 1/14, since the unit cell has seven rungs. This is much too small to be consistent with a HC periodicity of $5c_L$. Until we understand this discrepancy we really cannot reach any conclusions about the predictions of various proposed models regarding charge and spin ordering in these structures.

In this paper we solve this problem. We present an interpretation of the polarization dependent x-ray absorption (XAS) data which leads to a very different distribution of the holes between ladders and chains. We find that $n_L$ and $n_c$ are 2.8 and 3.2 for $x=0$, respectively. These values vary almost linearly with $x$, reaching $n_L=4.4$ and $n_c=1.6$ for $x=11$. As we show below, with these values the observed periodicities of the HC emerge quite naturally, as does an explanation in terms of simple resonance valence bond (RVB) physics for the absence of the HC with $\lambda=4c_L$, expected at $x=4$ but not observed. The end result is strong support for the model of hole pairing along rungs, predicted using simple *t-J* like models.[6]

The distribution of holes between the chains and ladders is essential in determining the answer for the problem we mentioned above, and for most physical properties. Like in high-$T_C$ cuprates, the holes are expected to enter into O 2*p* orbitals and to form spin compensated local bound states with a Cu 3*d* hole[14] referred to as Zhang-Rice (ZR) singlets.[15] Various experiments suggest that $n_L \approx 1$ and $n_c \approx 5$ at $x=0$, and provide evidence for a transfer of holes from the chains to the ladders upon Ca substitution. X-ray absorption measurements[16] find that $n_L$ ranges from 0.8 for $x=0$ to 1.1 for $x=12$. Optical conductivity data[17] find a range from 1 to 2.8, while $^{63}$Cu NMR studies[18] find a range from 1 to 3.5.

 

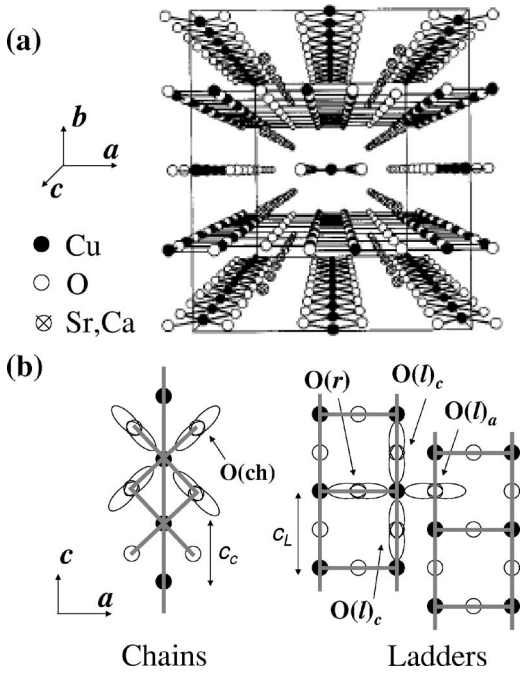


FIG. 1. (a) Crystal structure of $Sr_{14-x}Ca_xCu_{24}O_{41}$ (SCCO) viewed in perspective along the $c$ direction. (b) Sketch of the structure of chains and ladders. The orientation of the O $2p$ orbitals involved in the ZR singlets are indicated. The three different oxygen sites are identified for the ladder.

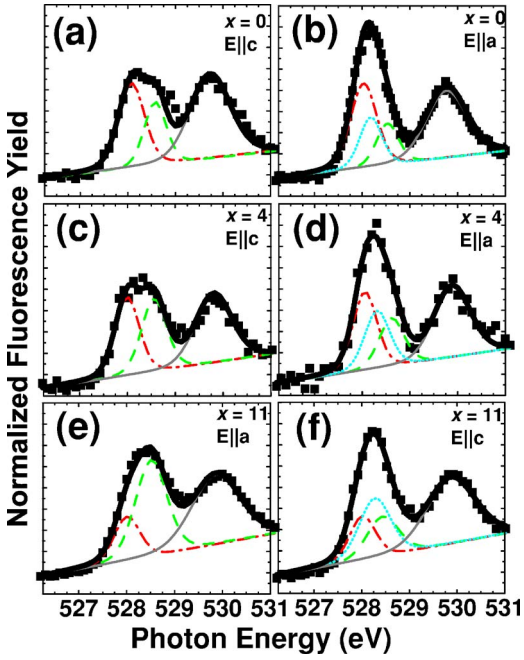


FIG. 2. (Color online) XAS spectra for E||$c$ (left panels) and E||$a$ (right panels) for $x=0$ [(a), (b)], $x=4$ [(c), (d)], and $x=11$ [(e), (f)]. Squares are the experimental data. The black solid lines show theoretical curves for the total fitting. The other lines are contributions from O(ch) (red dash-dotted lines), O($l$) (green dashed lines), O($r$) (cyan dotted lines), and the UHB (gray solid lines).

However, the optical conductivity and the NMR data analysis at $x=0$ are based on the neutron diffraction observation[19] of what was thought to be a superlattice reflection corresponding to a chain charge density wave (CDW) consistent with $n_c=5$, and thus $n_L=1$. More recent neutron studies[3,20] and analysis of the crystal structure by van Smaalen[21] have clearly shown that this peak is expected in the basic crystal structure and is therefore not evident for a CDW.

The only direct measurement of the hole density distribution comes from polarization-dependent XAS. This is also subject to interpretation, and the model used previously had unexplained discrepancies with regard to the polarization dependence. In Nücker *et al.*'s analysis[16] of the XAS data it is concluded that the holes are mainly concentrated on the chains. Their interpretation assumes that there are only two distinct O $1s$ pre-edge absorption energies, one (H1) corresponding to holes in the chains and the other (H2) to holes in the ladders. The H1 peak should be independent of the ac-plane polarization since the lobes of the O $2p$ orbitals involved in the chain ZR singlets are oriented at 45° to the $a$ and $c$ axes (see Fig. 1). The H2 peak should be strongly polarization dependent since the rung O and the leg O have different hole amplitudes. However, for $x=0$, XAS data shows that H1 is as strongly polarized as H2. In Ref. 16 it is argued that this effect is small and therefore is neglected.

## II. EXPERIMENT

Single crystals of SCCO were grown by traveling solvent floating zone techniques.[22] The surfaces were prepared in the manner described in Ref. 9. Polarization-dependent XAS measurements in the fluorescence detection mode were carried out on the soft x-ray undulator line X1B at the National Synchrotron Light Source. The energy resolution in the range of interest was about 200 meV. The spectra were corrected for incident flux variations and were normalized at about 70 eV above and 10 eV below the edge where the absorption is atomiclike and structureless.

## III. RESULT AND DISCUSSION

The $x=0$ spectrum shown in Figs. 2(a) and 2(b) is identical to that published in Ref. 16. Like them, we assign the lowest-energy structures to the holes doped in O $2p$ orbitals and the higher-energy structure at about 530 eV to transitions to the upper Hubbard band (UHB) or Cu $3d$ orbitals. These are followed by a broader structure due to transitions to unoccupied bands hybridized with O $2p$ and $3p$ states. The UHB structure is only weakly polarization dependent, as expected given the symmetry of the empty $d_{x^2-y^2}$ orbital. Since the point group symmetry for the ladder is not quite $D_{4h}$ (the four O surrounding a Cu are not identical, see Fig. 1) some polarization dependence remains. In addition, there is a strongly polarization dependent feature at lower energies, composed of at least two components. In Ref. 16, XAS data for $La_3Sr_{11}Cu_{24}O_{41.02}$ (with only three holes per unit cell) shows only one nearly polarization independent structure at the lower energy. As concluded there, this strongly suggests that the holes involved are almost solely on the chains, where

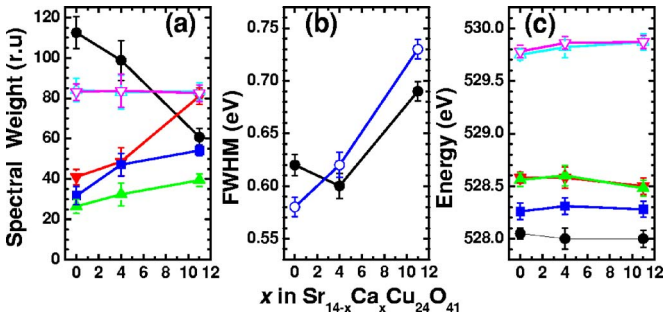


FIG. 3. (Color online) (a) Spectral weight, (b) full width at half maximum, and (c) energy of O(ch) (black solid circles), $O(l)_c$ (red solid down triangles), $O(l)_a$ (green solid up triangles), $O(r)$ (blue squares), UHB for E$\|c$ (cyan open up triangles), and UHB for E$\|a$ (magenta open down triangles) as function of $x$. Blue open circles are for oxygen ions in the ladders.

all O sites O(ch) are identical, and with $2p$ orbitals oriented to 45° (see Fig. 1).

In ladders, things are more complicated. There are two types of O sites: the rung sites, $O(r)$, coordinated by 2 Cu ions, and the leg sites, $O(l)$, coordinated by 3 Cu ions (see Fig. 1). The different coordination numbers result in different binding energies for the core $1s$ and valence $2p$ orbitals. Higher values are expected for the orbitals of $O(l)$, while those of $O(r)$ should be close to O(ch) which is also coordinated by 2 Cu ions. Moreover, each ladder ZR singlet involves one $O(r)_a$, two $O(l)_c$ from the leg, and one $O(l)_a$ from the leg of a neighboring ladder. The subscripts $a$ and $c$ refer to the polarization needed to observe O $1s \rightarrow 2p$ transitions. For $a$ polarization, transitions are possible for $O(r)_a$ and $O(l)_a$ at different energies, while for $c$ polarization, transitions are only possible from two identical $O(l)_c$, with energy close to that of $O(l)_a$.

To determine the spectroscopic parameters (peak position, width, and spectral weight), we performed a simultaneous least-square fit to all the measured spectra. The increasing background has been represented by an analytic function of a combination between Gaussian and linear backgrounds.[23] The fitting of the peaks is done to a sum of Gaussian and Lorentzian line shapes and we have found that the best fits are given by the ratio of about 80%. The spectral weight (SW), full width at half maximum (FWHM), and various energies are shown in Figs. 3(a)–3(c). The number of holes $n_L=6-n_c$ are determined from the spectral weights of the various absorption lines:

$$n_L = \frac{SW_{O(r)_a} + SW_{O(l)_a} + SW_{O(l)_c}}{SW_{O(r)_a} + SW_{O(l)_a} + SW_{O(l)_c} + SW_{O(ch)}}, \qquad (1)$$

where $SW_{O(ch)}$ is the total SW for both polarizations.

We start with $x=0$. XAS data and theoretical fits are shown in Figs. 2(a) and 2(b). For E$\|c$, the doped hole region has at least two structures. In our interpretation this is due to the energy difference between O(ch) and $O(l)_c$. For E$\|a$, the contribution of $O(l)_c$ should be replaced with that of $O(l)_a$ and $O(r)_a$, thus shifting more weight to the lower energy. This is indeed consistent with the data. In our fitting results, shown in Fig. 3, the energy of $O(r)_a$ is about 0.2 eV higher than that of O(ch), while the energy of $O(l)_c$ and $O(l)_a$ are roughly equal and about 0.5 eV higher than that of O(ch). The SW of the UHB is almost polarization independent. This shows that the ladder holes are distributed nearly isotropically among the 4 O involved in the ZR singlet, even though the symmetry is not the full $D_{4h}$. (If large deviations were found, the ZR picture would not be valid for the ladder holes.) The FWHM of O(ch), which is about 0.62 eV, is about 5% larger than the ones in the ladders. From Eq. (1), we find $n_L=2.8$ and $n_c=3.2$.

We continue the analysis for $x=4$. In Figs. 2(c) and 2(d) we show the fitting for E$\|c$ and E$\|a$ data, respectively. Again, the SW in the UHB is almost polarization independent, as shown in Fig. 3(a), while the energies of the various O sites are close to the $x=0$ values, see Fig. 3(c), consistent with our understanding of the polarization dependent XAS. From Eq. (1) we find that here $n_L=3.4$ and $n_c=2.6$.

Figures 2(e) and 2(f) show our XAS data for $x=11$. (The maximum HC intensity occurs at $x=11$ where the wave vector is closest to $3c_L$.[10]) In Ref. 16 it is claimed that here, the UHB is strongly polarization dependent while the O doped hole pre-edge region is almost polarization independent. Our results show an opposite behavior, such as for samples with smaller $x$. In fact, the shape and the intensity of the hole doped and UHB peaks of Ref. 16 are similar to ours, and can be made to coincide by rescaling. We conclude that the difference is due to the method used in the normalization of the data. The fit of the polarization dependent XAS for $x=11$ is more difficult than for $x=0$ or 4. The problem is not statistical noise, but rather the structural peaks themselves.

We see in Figs. 2(e) and 2(f) that there is no clear evidence for multiple peaks in the doped hole regime because the energy resolution is too poor to resolve the peaks. We therefore use the $x=0$ results as input for the fitting. The fits are shown in Figs. 2(e) and 2(f). As before, we find that the SW of UHB is almost polarization independent and the energies of the various O sites remain close to the $x=0$ values (see Fig. 3), validating our interpretation. We find $n_L=4.4$ and $n_c=1.6$. It is important to mention that these results depend strongly on the energy of O(ch). For example, varying it by 0.05 eV changes $n_L$ by about 0.5. This is due to an instability in the fitting process caused by the close proximity of peaks in the pre-edge region [the energy of O(ch) falls close to the leading edge of the hole-doped peak]. This is why the $x=0$ spectrum provides an important reference and the energy calibration has to be correct.

We now analyze some possible scenarios of the hole distribution in the ladder, for these $n_L$ values. We also consider the connection to the wavelengths $\lambda_{HC}=3c_L$ ($x=11$) and $5c_L$ ($x=0$) of the recently discovered HC.[9,10] First, density matrix renormalization group (DMRG) calculations for a single ladder[6] found that holes prefer to pair along the rungs, resulting in a charge density wave shown pictorially in Fig. 4(a), part i. For periodicity $\lambda_{HC}=Nc_L$, the number of holes in ladder $n_L$ should be 14/N, i.e., $n_L=2.8$ if $N=5$, $n_L=3.5$ if $N$

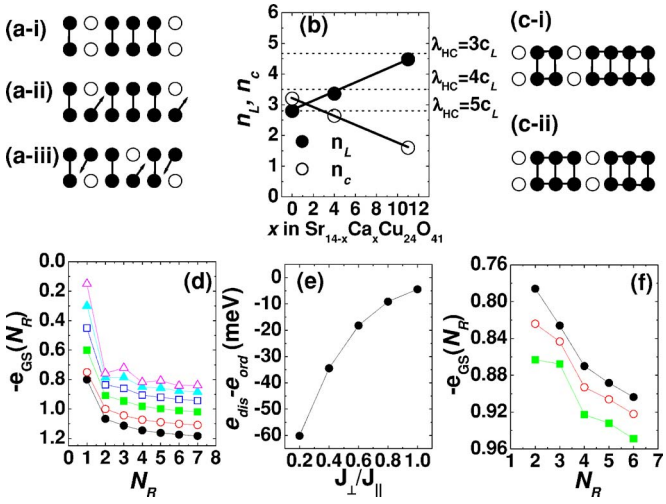


FIG. 4. (Color online) [(a), part i to part iii] Scenarios for the ladder hole distribution in a HC with $\lambda=4c_L$. Filled (open) circles represent electrons (holes). Arrows indicate the spin of unpaired electrons. (b) The estimated number of holes in the ladders (filled circles) and the chain (open circles) per unit cell. Dashed lines show the number of holes for scenario [(a), part i], for $\lambda_{HC}/c_L=3$, 4, and 5. [(c), part i] Disordered and [(c), part ii] ordered hole arrangement corresponding to $\lambda_{HC}=4c_L$. The disordered state has equal numbers of two-rung and four-rung spin plaquettes. (d) GS energy per rung, in units of $J_\parallel$, as a function of the number of rungs in the spin plaquette. Black solid circles, red open circles, green solid squares, blue open squares, cyan solid triangles, and magenta open triangles are results for $J_\perp/J_\parallel=1.2$, 1.0, 0.8, 0.6, 0.4, and 0.2, respectively. (e) $e_{dis}-e_{ord}$ as a function of $J_\perp/J_\parallel$, for $J_\parallel=130$ meV (see text for details). (f) $e_{GS}(N_R)$ vs $N_R$ for $J_\perp/J_\parallel=0.4$ and $J_{\text{ring}}/J_\parallel=-0.1$, 0, and 0.1 (black solid circles, red open circles, and green solid squares, respectively).

$=4$, and $n_L=4.67$ if $N=3$. These values are very close to our XAS estimates, as shown in Fig. 4(b). Surprisingly, however, the $\lambda_{HC}=4c_L$ HC, which is predicted by DMRG[6,7] to be a stable phase, is not observed in RSXS.[10] While the study of this discrepancy is ongoing, a possible explanation is proposed below. Another hole distribution consistent with these $\lambda_{HC}$ values, not involving pairing, and also discussed in Ref. 6, is single rung bond-centered holes which is shown in Fig. 4(a), part ii. Since $n_L$ for this case is halved, this model does not match our XAS results. In a third scenario proposed in Ref. 6, the holes could be site centered, alternating between the two legs as shown in Fig. 4(a), part iii. While this matches the $n_L$ values, it requires an odd number of undoped rungs in the HC unit cell and is therefore inconsistent with the observed $N=3$ and $N=5$ HC. We conclude that our results support the scenario of holes paired along the rungs.

Assuming rung-paired holes, a minimal model of the doped ladder is an antiferromagnetic Heisenberg Hamiltonian plus a cyclic four spin exchange term:[24,25]

$$\mathcal{H}=J_\parallel\sum_{\substack{n=1\\ \alpha=1,2}}^{N_R-1}\mathbf{S}_{\alpha,n}\cdot\mathbf{S}_{\alpha,n+1}+J_\perp\sum_{n=1}^{N_R}\mathbf{S}_{1,n}\cdot\mathbf{S}_{2,n}+\mathcal{H}_{\text{ring}}.$$

Here, $N_R=N-1$ is the number of undoped rungs per HC unit cell corresponding to a periodicity $\lambda_{HC}=Nc_L$. $\alpha=1$, 2 indexes spins on the two legs, and $J_\perp$ and $J_\parallel$ are exchange couplings along the rung and leg, respectively. We assume no coupling between spins on opposite sides of rungs occupied by paired holes. The ring exchange is a sum over all spin plaquettes of the HC unit cell, $\mathcal{H}_{\text{ring}}=J_{\text{ring}}\sum_{n=1}^{N_R-1}\left[\frac{1}{4}+\mathcal{H}_{n,\text{ring}}\right]$, where the four-spin cyclic exchange for each spin plaquette is

$$\begin{aligned}\mathcal{H}_{n,\text{ring}}=&\,\mathbf{S}_{1,n}\cdot\mathbf{S}_{1,n+1}+\mathbf{S}_{2,n}\cdot\mathbf{S}_{2,n+1}+\mathbf{S}_{1,n}\cdot\mathbf{S}_{2,n+1}+\mathbf{S}_{2,n}\cdot\mathbf{S}_{1,n+1}\\&+\mathbf{S}_{1,n}\cdot\mathbf{S}_{2,n}+\mathbf{S}_{1,n+1}\cdot\mathbf{S}_{2,n+1}+4[(\mathbf{S}_{1,n}\cdot\mathbf{S}_{2,n})\\&\times(\mathbf{S}_{1,n+1}\cdot\mathbf{S}_{2,n+1})+(\mathbf{S}_{1,n}\cdot\mathbf{S}_{1,n+1})(\mathbf{S}_{2,n}\cdot\mathbf{S}_{2,n+1})\\&-(\mathbf{S}_{1,n}\cdot\mathbf{S}_{2,n+1})(\mathbf{S}_{2,n}\cdot\mathbf{S}_{1,n+1})].\end{aligned}$$

We use exact diagonalization to find the ground state for various $N_R$ values. The ground-state (GS) energy per rung, $e_{GS}(N_R)=E_{GS}(N_R)/N_R$, is shown in Fig. 4(d) for various ratios of $J_\perp/J_\parallel$ and $J_{\text{ring}}=0$. The value of $J_\perp/J_\parallel$ is not known accurately, but is believed to be between 0.5 and 1.13.[18,27–31] An even-odd oscillation is observed for small $N_R$ and $J_\perp/J_\parallel<1$, favoring $N_R=2$ and 4 ($\lambda_{HC}=3,5c_L$). The origin of this oscillation is simple. The limit $J_\perp/J_\parallel\to 0$ corresponds to two AFM chains weakly coupled along the rungs. For even $N_R$, to first-order spins on each leg pair in a RVB-like state, and $E_{GS}$ is low. For odd $N_R$ and $J_\perp=0$, each leg has an unpaired spin. A small but finite $J_\perp$ allows them to pair in a singlet across a rung, however this state has a significantly increased $E_{GS}$. In the limit $J_\perp\gg J_\parallel$, the GS consists of spin singlets along the rungs and the parity of $N_R$ is irrelevant. At large $N_R$, $e_{GS}$ converges to the bulk value. This even-odd oscillation provides a possible explanation for the absence of a HC with $N_R=3$ ($\lambda_{HC}=4c_L$). This HC costs an energy $e_{ord}=6e_{GS}(3)$ per two HC unit cells [see Fig. 4(c), part ii]. A disordered phase, at the same doping, has equal numbers of $N_R=2$ and $N_R=4$ plaquettes and an energy $e_{dis}=2e_{GS}(2)+4e_{GS}(4)$ for the same length [see Fig. 4(c), part i]. If $e_{dis}<e_{ord}$, the HC phase is unstable. For $J_\parallel=130$ meV, we plot $e_{dis}-e_{ord}$ in Fig. 4(e), showing that the disordered phase is energetically favorable, especially for lower values of $J_\perp/J_\parallel$.

We have also studied the effect of $\mathcal{H}_{\text{ring}}$ on $E_{GS}$. Such terms appear in fourth order perturbation expansions in the strong coupling limit of the Hubbard model[24] and are known to play an important role for Wigner crystals and $^3$He solid. Typical results for $e_{GS}(N_R)$ are shown in Fig. 4(f), for $J_\perp/J_\parallel=0.56$ and $J_{\text{ring}}/J_\parallel=-0.1$, 0, and 0.1.[26] Since the sign of the ring exchange and superexchange should be the same,[24] it follows that a large $J_{\text{ring}}$ suppresses the even-odd effect. For example, for $J_\perp/J_\parallel=0.56$, $e_{dis}-e_{ord}$ increases from $-20.8$ meV if $J_{\text{ring}}=0$, to $-12.5$ meV if $J_{\text{ring}}/J_\parallel=0.1$. We conclude that for reasonable values of $J_\perp$, $J_\parallel$, and $J_{\text{ring}}$ this simple model offers a possible explanation for the absence of the $\lambda_{HC}\sim 4c_L$ HC. An accurate determination of the exchange couplings is needed before the issue can be settled.

## IV. CONCLUSION

In conclusion, we propose an interpretation of polarization dependent XAS for SCCO, which gives very different results for the distribution of the holes among chains and ladders in this compound compared to those used in literature. These values are in excellent agreement with hole densities on the ladders needed to observe the HC with $\lambda_{HC}=3c_L$ and $5c_L$, if the holes pair along the rungs of the ladders. Hole pairing along the rungs is also supported by numerical simulations. We also give a possible explanation for the absence of the HC with $\lambda_{HC}=4c_L$ in terms of RVB physics. Thus, this interpretation is fully consistent with RSXS data regarding the various HC observed in these compounds. These results offer strong support for a pairing of holes along the rungs of the two-leg ladders.

## ACKNOWLEDGMENTS

We acknowledge helpful discussions with I. Affleck, A. Sandvik, G. Blumberg, and J. Zaanen. This work was supported by The Netherlands Organization for Fundamental Research on Matter (FOM), the Helmholtz Association Contract No. VH-FZ-007, the German Research Foundation Contract No. DFG Ru 773/2-3, the 21st Century COE program of the Japan Society for Promotion of Science, and the Office of Basic Energy Sciences, U.S. Department of Energy under Grant No. DE-FG02-06ER46285, with use of the NSLS supported under Contract No. DE-AC02 98CH10886. M.B and G.A.S were supported by the Natural Sciences and Engineering Research Council of Canada, the Canadian Foundation for Innovation, and the Canadian Institute for Advanced Research.

[1] E. M. McCarron, M. A. Subramanian, J. C. Calabrese, and R. L. Harlow, Mater. Res. Bull. **23**, 1355 (1988).
[2] T. Siegrist, L. F. Schneemeyer, S. A. Sunshine, and J. V. Waszczak, Mater. Res. Bull. **23**, 1429 (1988).
[3] J. Etrillard, M. Braden, A. Gukasov, U. Ammerahl, and A. Revcolevschi, Physica C **403**, 290 (2004).
[4] E. Dagotto, J. Riera, and D. Scalapino, Phys. Rev. B **45**, 5744 (1992).
[5] E. Dagotto and T. M. Rice, Science **271**, 618 (1996).
[6] S. R. White, I. Affleck, and D. J. Scalapino, Phys. Rev. B **65**, 165122 (2002).
[7] S. T. Carr and A. M. Tsvelik, Phys. Rev. B **65**, 195121 (2002).
[8] M. Uehara, T. Nagata, J. Akimitsu, H. Takahashi, N. Môri, and K. Kinoshita, J. Phys. Soc. Jpn. **65**, 2764 (1996).
[9] P. Abbamonte, G. Blumberg, A. Rusydi, A. Gozar, P. G. Evans, T. Siegrist, L. Venema, H. Eisaki, E. D. Isaacs, and G. A. Sawatzky, Nature (London) **431**, 1078 (2004).
[10] A. Rusydi, P. Abbamonte, H. Eisaki, Y. Fujimaki, G. Blumberg, S. Uchida, and G. A. Sawatzky, Phys. Rev. Lett. **97**, 016403 (2006).
[11] J. M. Tranquada, J. D. Axe, N. Ichikawa, A. R. Moodenbaugh, Y. Nakamura, and S. Uchida, Phys. Rev. Lett. **78**, 338 (1997).
[12] G. S. Uhrig, K. P. Schmidt, and M. Grüninger, Phys. Rev. Lett. **93**, 267003 (2004).
[13] J. M. Tranquada, H. Woo, T. G. Perring, H. Goka, G. D. Gu, G. Xu, M. Fujita, and K. Yamada, Nature (London) **429**, 534 (2004).
[14] H. Eskes and G. A. Sawatzky, Phys. Rev. Lett. **61**, 1415 (1988).
[15] F. C. Zhang and T. M. Rice, Phys. Rev. B **37**, 3759 (1988).
[16] N. Nücker, M. Merz, C. A. Kuntscher, S. Gerhold, S. Schuppler, R. Neudert, M. S. Golden, J. Fink, D. Schild, S. Stadler, V. Chakarian, J. Freeland, Y. U. Idzerda, K. Conder, M. Uehara, T. Nagata, J. Goto, J. Akimitsu, N. Motoyama, H. Eisaki, S. Uchida, U. Ammerahl, and A. Revcolevschi, Phys. Rev. B **62**, 14384 (2000).
[17] T. Osafune, N. Motoyama, H. Eisaki, and S. Uchida, Phys. Rev. Lett. **78**, 1980 (1997).
[18] K. Magishi, S. Matsumoto, Y. Kitaoka, K. Ishida, K. Asayama, M. Uehara, T. Nagata, and J. Akimitsu, Phys. Rev. B **57**, 11533 (1998).
[19] M. Matsuda, K. Katsumata, H. Eisaki, N. Motoyama, S. Uchida, S. M. Shapiro, and G. Shirane, Phys. Rev. B **54**, 12199 (1996).
[20] M. Braden, J. Etrillard, A. Gukasov, U. Ammerahl, and A. Revcolevschi, Phys. Rev. B **69**, 214426 (2004).
[21] S. van Smaalen, Phys. Rev. B **67**, 026101 (2003).
[22] N. Motoyama, T. Osafune, T. Kakeshita, H. Eisaki, and S. Uchida, Phys. Rev. B **55**, R3386 (1997).
[23] C. T. Chen, F. Sette, Y. Ma, M. S. Hybertsen, E. B. Stechel, W. M. C. Foulkes, M. Schluter, S.-W. Cheong, A. S. Cooper, L. W. Rupp, Jr., B. Batlogg, Y. L. Soo, Z. H. Ming, A. Krol, and Y. H. Kao, Phys. Rev. Lett. **66**, 104 (1991).
[24] M. Takahashi, J. Phys. C **10**, 1289 (1977).
[25] S. Brehmer, H.-J. Mikeska, M. Müller, N. Nagaosa, and S. Uchida, Phys. Rev. B **60**, 329 (1999).
[26] R. S. Eccleston, Masatomo Uehara, Jun Akimitsu, Hiroshi Eisaki, Naoki Motoyama, and Shin-ichi Uchida, Phys. Rev. Lett. **81**, 1702 (1998).
[27] T. Imai, K. R. Thurber, K. M. Shen, A. W. Hunt, and F. C. Chou, Phys. Rev. Lett. **81**, 220 (1998).
[28] K. I. Kumagai, Sigenori Tsuji, Masatsune Kato, and Yoji Koike, Phys. Rev. Lett. **79**, 1992 (1997).
[29] P. Carretta, S. Aldrovandi, R. Sala, P. Ghigna, and A. Lascialfari, Phys. Rev. B **56**, 14587 (1997).
[30] M. Takigawa, Naoki Motoyama, Hiroshi Eisaki, and Shinichi Uchida, Phys. Rev. B **57**, 1124 (1998).
[31] A. Gozar, G. Blumberg, B. S. Dennis, B. S. Shastry, N. Motoyama, H. Eisaki, and S. Uchida, Phys. Rev. Lett. **87**, 197202 (2001).